JARQ 53 (3), 181-190 (2019) https://www.jircas.go.jp

Assessment of Floodwater Behavior in Van Coc Lake, Hanoi in Event of Emergency Situation

Sai Hong ANH[1,3], Toshinori TABATA[2]*, Kazuaki HIRAMATSU[2], Masayoshi HARADA[2] and Le Viet SON[3]

[1] Department of Agro-environmental Sciences, Graduate School of Bioresources and Bioenvironmental Sciences, Kyushu University (Fukuoka, Fukuoka 812-8581, Japan)
[2] Department of Agro-environmental Sciences, Faculty of Agriculture, Kyushu University (Fukuoka, Fukuoka 812-8581, Japan)
[3] Division for Water Resources Planning for the North Region, Institute of Water Resources Planning (Hanoi, Vietnam)

Abstract

Van Coc Lake located in the Dan Phuong and Phuc Tho, Hanoi, Vietnam, has an area of 30.83 km^2. It is usually dry and includes arable land and residential areas. However, to protect Hanoi City from catastrophic floods, in emergency situations, it receives the floodwater from the Red River as a regulating reservoir and drains the floodwater to the downstream Day River through the Day Weir. We performed numerical simulations to assess the movement of floodwater in this lake and evaluated the impact of floodwater on its residential areas. A two-dimensional depth-integrated hydrodynamic model was constructed to simulate inundation in this lake. The model was validated and the effects of Manning's coefficient of roughness were examined. In case of emergency, it has to receive an inflow of 2,500 m^3/s into the area. Inflow rates of 1,200 and 600 m^3/s were also examined to compare the results. The simulation results indicate that this lake was entirely inundated in 13, 28, and 56 h by inflow rates of 2,500, 1,200, and 600 m^3/s, respectively. Between 66% and 99% of residential areas were inundated. The areas with highest velocity were primarily focused behind the gate with a velocity of 1.5-1.8 m/s.

Discipline: Agricultural engineering
Additional key words: Day Weir, Red River, two-dimensional depth-integrated model, flood disaster

Introduction

Flooding is the most frequent natural disaster in the world (IFRC 2015), and it causes huge damage to the economy and to the people. The dangers of floods and their terrible consequences have been recorded in many places in the world. Simulating the behavior of floodwater plays an important role in national decision making regarding flood prevention, risk assessment, and management (An et al. 2015, Caviedes-Voullième et al. 2014).

The Red River is the largest river in northern Vietnam with three main tributaries, namely, the Da, the Thao, and the Lo. The river runs through the Vietnamese capital, Hanoi, and has a huge economic and historical value. According to the ASEAN Coordinating Centre for Humanitarian Assistance on Disaster Management and the Japan International Cooperation Agency (2015), flooding is a serious problem in the Red River Delta. In 1971, a huge flood occurred in many provinces, including the capital (Hanoi), in the Red River Delta. This flood was one of the 10 worst floods of the 20th century. Dangerous weather in the area led to heavy rains, dike breakage, and significant increase of the water levels in the river system. A total of 100,000 people died from this disaster (NOAA 1993). In 2008, there was a major flood in Hanoi and its surrounding areas that caused damage of up to 400 million US dollars in the economy (AHA Centre and JICA 2015). Furthermore, the water level during the flooding season from June to October has become increasingly higher because of deforestation and sediment deposition in the upstream parts of the river. Hydraulic structures, such as dams and weirs, were also being degraded in Vietnam (RRBO 2015). Moreover,

*Corresponding author: e-mail ttabata@bpes.kyushu-u.ac.jp
Received 29 May 2018; accepted 30 October 2018.

prediction of floodwater has become more difficult than before because of climate change and sea level rise (MONRE 2012). Consequently, the Vietnamese Government and other stakeholders have devoted significant efforts to predicting and mitigating flooding in the Red River (Vietnamese Government 2011).

Van Coc Lake, located in the Dan Phuong District and Phuc Tho District of Hanoi City, Vietnam has an area of 30.83 km^2. It is usually dry and include arable land and residential areas (see Figure 1 for a location map of Van Coc Lake). In order to protect the City of Hanoi from catastrophic floods in emergency situations, the Vietnamese Government at the time of this study was considering diverting floodwater from the Red River into Van Coc Lake. In this scenario, Van Coc Lake will receive 2,500 m^3/s of floodwater from the Red River through the Van Coc [sluice] Gate to act as a regulating reservoir and drain the water to the downstream Day River through the Day Weir (Vietnamese Government 2014, 2016). Assessing the impact of floods on the residential areas is essential and a comprehensive assessment of the hydraulic behavior in the area is also very important.

In this study, we performed numerical simulations to assess the behavior of floodwater in Van Coc Lake and investigate the impact of floodwater on its residential areas. A two-dimensional depth-integrated hydrodynamic model was constructed to simulate the inundation of water in Van Coc Lake in the case of the different inflow rates from the Van Coc Gate, that is located adjacent to the Red River. The model was validated with the observed water level in the Red River and the effects of the Manning's coefficient of roughness on the floodwater behavior were also examined.

Materials and Methods

1. Study area

Van Coc Lake is a regulating reservoir and receives floodwater through Van Coc Gate from the Red River in

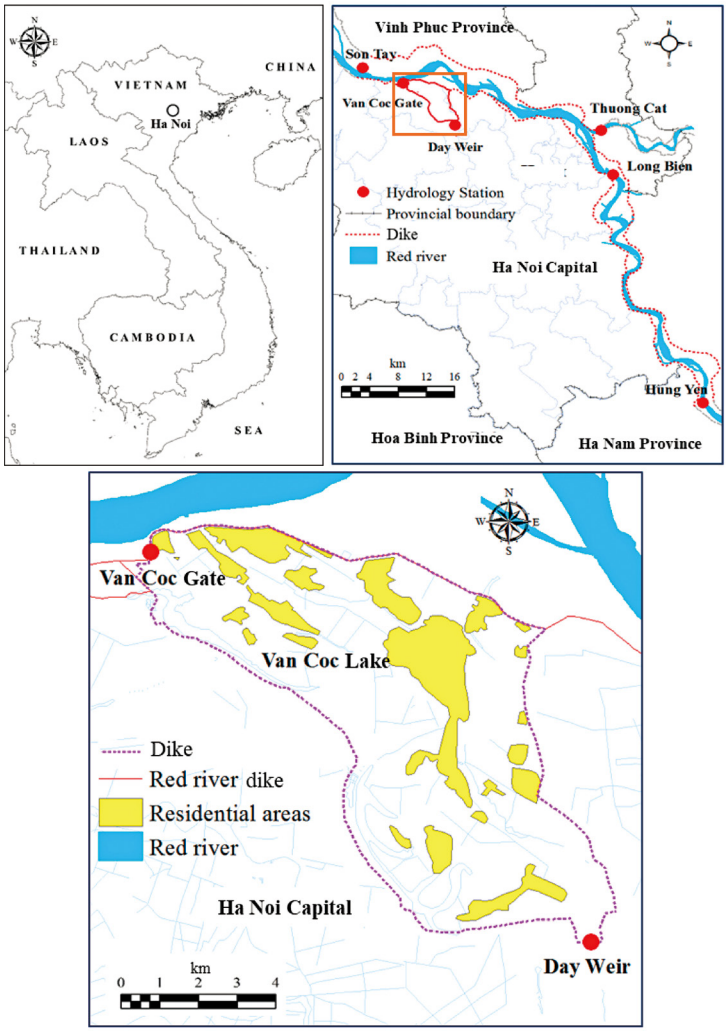

Fig. 1. The targeted areas for simulations

emergency situations. Van Coc Gate will divert floodwater from the Red River into Van Coc Lake to reduce the floodwater pressure on the Red River dike system to protect the City of Hanoi. It has previously been used once for this purpose in 1971 to protect Hanoi from flooding, but there was no recorded profile at that time. Therefore, our model was validated at the Long Bien Station in the Red River before applying it to Van Coc Lake. Figure 1 depicts the study areas for the model validations and inundation simulations using the two-dimensional depth-integrated hydrodynamic model. The Red River model was built to cover an area of 395.2 km^2, and comprises 158,061 grid cells, each with a resolution of 50 m. Profiles observed at Long Bien in 2014 were used as validation data. Once validated, the model was applied to simulate the inundation in the Van Coc Lake area; that is, an area of 30.8 km^2 and 12,333 grid cells with a resolution of 50 m.

Topographic data were surveyed by the Institute of Water Resources Planning, the Ministry of Agriculture and Rural Development, Vietnam in 2011 and 2013. The natural neighbor technique in ESRI's ArcGIS software was utilized for interpolating topographic surfaces from the available points to calculate the elevation for each cell. Figure 2 shows the elevation of Van Coc Lake after integrating the final elevation for each cell with the land use map of residential and cultivated areas.

The Vietnamese Government (2016) set out an emergency plan for Van Coc Lake to receive the floodwater from the Red River to protect the City of Hanoi from flooding. In this emergency plan, the Van Coc Gate has to receive an inflow of 2,500 m^3/s in case of emergency situations. Hence, we simulated inflow scenarios of 2,500 m^3/s, as well as 1,200 m^3/s and 600 m^3/s to compare the results.

2. Hydrodynamic model

Two-dimensional models (Bellos and Tsakiris 2015, Hu and Kot 1997, Tabata et al. 2013) and three-dimensional hydrodynamic models (Abedini et al. 2010, Wu and Lin 2015) have been used to simulate water flow dynamics. In this study, the research area is a floodplain and the study therefore focuses on the behavior of floodwater, wherein the horizontal velocities are far greater than the vertical velocities; moreover, three-dimensional models are time consuming. Therefore, we applied a two-dimensional depth-integrated model to simulate the behavior of floodwater in the area. The shallow water equations used in this study are as follows:

Continuity equation:

$$\frac{\partial \eta}{\partial t}+\frac{\partial}{\partial x}\{Uh\}+\frac{\partial}{\partial y}\{Vh\}=0 \quad (1)$$

Momentum equations in the x and y directions:

$$\frac{\partial U}{\partial t}+U\frac{\partial U}{\partial x}+V\frac{\partial U}{\partial y}$$
$$=fV-g\frac{\partial \eta}{\partial x}+\nu_h\left(\frac{\partial^2 U}{\partial x^2}+\frac{\partial^2 U}{\partial^2 y}\right)-\frac{gn^2U\sqrt{U^2+V^2}}{h^{4/3}} \quad (2)$$

$$\frac{\partial V}{\partial t}+U\frac{\partial V}{\partial x}+V\frac{\partial V}{\partial y}$$
$$=-fU-g\frac{\partial \eta}{\partial y}+\nu_h\left(\frac{\partial^2 V}{\partial x^2}+\frac{\partial^2 V}{\partial^2 y}\right)-\frac{gn^2V\sqrt{U^2+V^2}}{h^{4/3}} \quad (3)$$

where U and V are the depth-averaged horizontal velocity components in the x and y directions (m/s), η is the water level (m), t is time (s), h is the water depth (m), f is the Coriolis force (1/s), g is the gravitational acceleration (m/s^2), n is Manning's coefficient of roughness (s/m$^{1/3}$), and ν_h is the coefficient of eddy viscosity (m^2/s). In this paper,

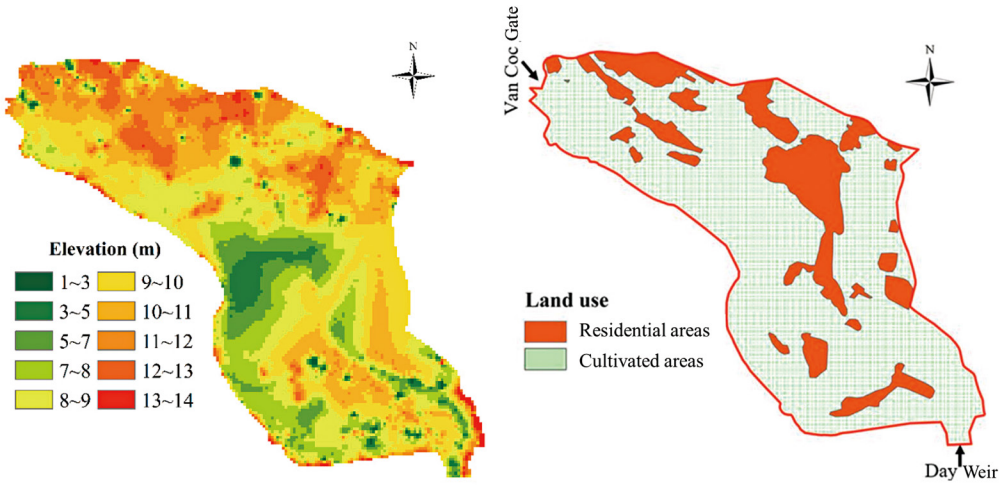

Fig. 2. The elevation and land use in Van Coc Lake

v_h was calculated using equation (4), as proposed by Smagorinsky (1963).

$$v_h = \frac{1}{2} S_m A_G \left\{ \left(\frac{\partial U}{\partial x} \right)^2 + \frac{1}{2} \left(\frac{\partial V}{\partial x} + \frac{\partial V}{\partial y} \right)^2 + \left(\frac{\partial V}{\partial y} \right)^2 \right\}^{1/2} \quad (4)$$

where S_m is the Smagorinsky coefficient, and A_G is the area of each mesh point (m^2).

The basic parameters are defined in Table 1. The Manning coefficient of roughness n in Table 1 is explained more fully in item 4 of this section. The leapfrog finite difference method was applied to calculate the governing equations on the staggered mesh system. The model was run with a time step of Δt= 2.0 (s), in which the water level and velocity were calculated alternately.

A wetting and drying scheme of Uchiyama (2004) was used to identify the wet and dry areas at each time step.

3. Boundary conditions

The observed profiles collected in 2014 by the Institute of Water Resources Planning in the Red River area were used to validate the model. In the model validation scenarios, the discharge at the Son Tay Station and the observed water levels at the Thuong Cat and Hung Yen stations were used as the boundary conditions (Figures 3, 4). Furthermore, the observed water levels at the Long Bien Station were used to compare the results between calculated and observed profiles.

In the inundation simulations, an inflow of 2,500 m^3/s was used at the Van Coc Gate as the boundary condition; inflow rates of 1,200 m^3/s and 600 m^3/s at the same gate were also simulated to compare these results. During this study, the Day Weir was closed.

4. Manning's coefficient of roughness

Manning's coefficient of roughness is an important

Table 1. The model parameters

Parameter	Value
Δt(s)	2.0
Δx=Δy (m)	50.0
S_m	0.2
n (s/m$^{1/3}$)	0.025-0.172
A_G(m^2)	2500.0
f(1/s)	5.24x10^{-5}
g (m/s^2)	9.8

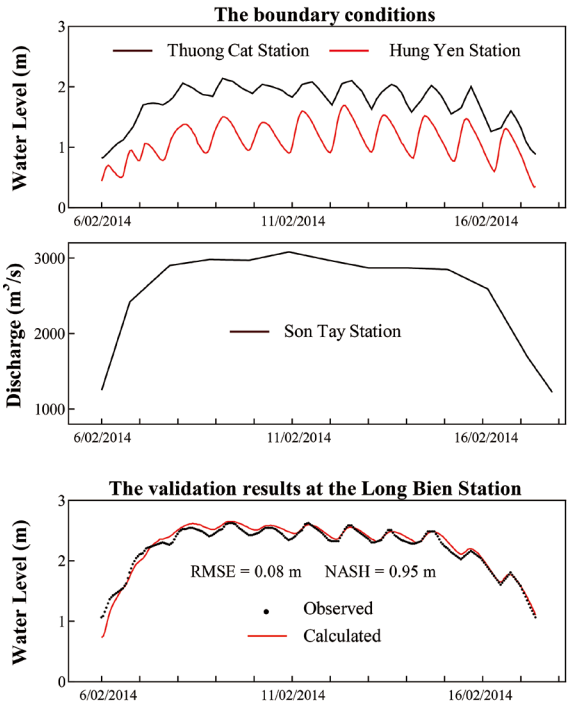

Fig. 3. The calculated and observed water levels at the Long Bien Station and the boundary conditions of the water levels at the Thuong Cat and Hung Yen Stations and the discharge at the Son Tay Station from February 6th to February 17th, 2014 in the Red River

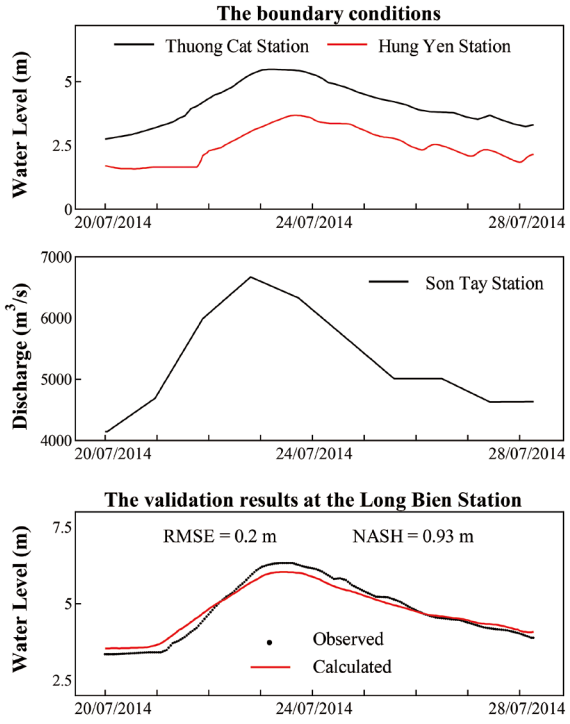

Fig. 4. The calculated and observed water levels at the Long Bien Station and the boundary conditions of the water levels at the Thuong Cat and Hung Yen Stations and the discharge at the Son Tay Station from July 20th to July 28th, 2014 in the Red River

parameter that represents the resistance of flow in floodplains and river channels. Flood risk is higher when Manning's coefficient is higher in the upstream area (De Doncker et al. 2009). Differences in *n* imply a difference in both the water level and the flow velocity. Constant values of *n* have been used for the entire floodplain area by some researchers (Kvocka et al. 2015, Pinho et al. 2015). However, the performance of hydraulic models improves when *n* is better estimated (Kalyanapu et al., 2009). Moreover, the study area features a mixture of land uses, which affect differently the water level and velocity. Therefore, *n* was examined by defining two cases: Case 1: n = 0.035-0.172 s/m$^{1/3}$ depending on the vegetation, obstructions, and residential areas; and Case 2: n = 0.035 s/m$^{1/3}$ for all the meshes (Brunner 2010, Bricker et al. 2015). A detailed representation of *n* in Case 1 is shown in Figure 5, in which the values of 0.035 and 0.172 s/m$^{1/3}$ were used for the cultivated and residential areas, respectively. The two cases of *n* were applied to the three inflow scenarios at the Van Coc Gate. In the model validation, *n* for the channel, cultivated, and residential areas was defined as 0.025, 0.035, and 0.172 s/m$^{1/3}$, respectively.

Results and discussion

1. Model validation

The validation results of the model are showed in Table 2 and Figures 3 and 4 for two validation periods from February 6th to February 17th, 2014, and from July 20th to July 28th, 2014. The accuracy of the model was assessed using the root-mean-square error (RMSE) and Nash-Sutcliffe model efficiency coefficient (NASH), as is shown in Figures 3 and 4. Obviously, the model performs well: values of RMSE and NASH of 0.08 m and 0.95 for the first period and 0.2 m and 0.93 for the second period indicate the good agreement between the observed and calculated water levels. Figures 3 and 4 also show the good agreement between the calculated and observed water level at Long Bien Station. It was concluded that the two-dimensional depth-integrated model developed here could be accurately utilized for the simulations in Van Coc Lake.

2. Relationship between time and water depth

Figure 6 shows the velocity vectors and land area in the targeted area at 2 h and 50 min after the start of the inflow discharge of 2,500 m^3/s at the Van Coc Gate in Case 1 (n of 0.035-0.172 s/m$^{1/3}$). Figure 7 presents a comparison chart of the relationship between the time and the water depth in front of the Day Weir with two different cases of *n* and three inflow discharges at the Van Coc Gate. The water depth changes in front of the Day Weir depending on *n* (Case 1: n = 0.035-0.172 s/m$^{1/3}$ and Case 2: n = 0.035 s/m$^{1/3}$) and the inflow rates at the Van Coc Gate.

The floodwater in the scenario with an inflow of 2,500 m^3/s reached the Day Weir after 4 h. In the following hour, the water depth in Cases 1 and 2 rose to 1.2 m and 1.57 m, respectively. At the fifth hour, the water depths significantly increased to 2.24 m in Case 1 and 2.26 m in Case 2. The water depth rose to 4.9 m, which

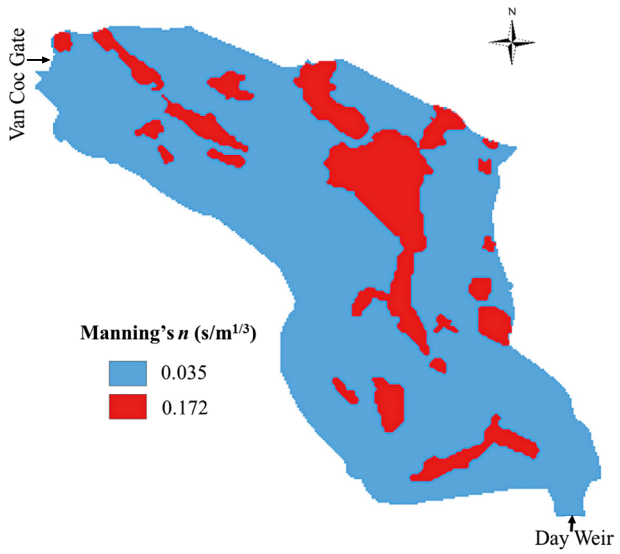

Fig. 5. The Manning's coefficient *n* of Case 1, in which the values of 0.035 and of 0.172 s/m$^{1/3}$ were used for the cultivated and residential areas, respectively

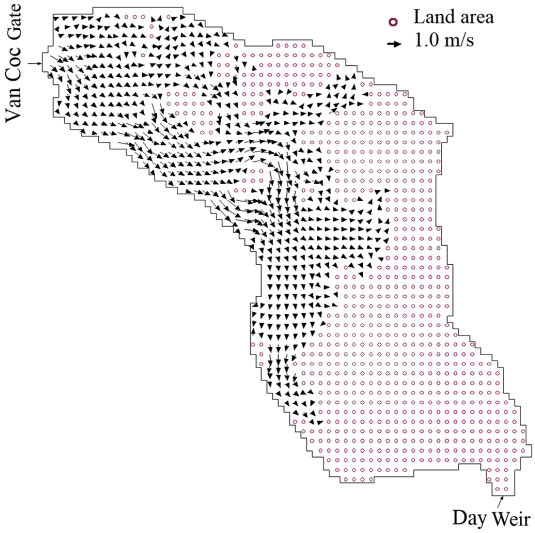

Fig. 6. Velocity vectors and land area in the study area after 2 h and 50 min with the inflow discharge of 2,500 m^3/s at the Van Coc Gate in Case 1 (Manning's *n* of 0.035-0.172 s/m$^{1/3}$)

corresponds to the maximum weir height, after 13 h and 41 min in both Cases. The maximum difference in water depth between the two Cases was 0.37 m at the fourth hour. From this point onward, the difference decreased to become insignificant, and fluctuated between 4 cm and 0 cm from the 5th to the 14th h.

For the 1,200 m^3/s inflow scenario, the water depth in front of the Day Weir changed slowly. The water depth did not increase and remained at 0.03 m during the first 6 h in Case 1 and the first 5 h in Case 2. In Case 1, the water depth quickly rose from 0 m at the sixth hour to 1.6 m at the seventh hour. In Case 2, there is a significant increase of water depth to 0.52 m at the sixth hour, which was 0.49 m higher than water depth in Case 1 also at the sixth hour. However, by the seventh hour the difference had decreased to 0.14 m. From the 8th to the 29th h, the hourly water depth differed only slightly in both cases and fluctuated between 3 cm and 0 cm. The water depth slowly increased to reach a peak of 4.9 m after 28 h in both cases.

For the 600 m^3/s inflow model, the water depth did not change and remained at 0 m during the first 10 h in Case 1 and during the first nine hours in Case 2, before significantly increasing in the next hour to 1.29 m in Case 1 and 1.07 m in Case 2. At the 11th h, the water depth in Case 1 was 0.21 cm lower than the water depth of Case 2. The differences in water depth during the period between the 12th and 18th h decreased to 2 cm from 5 cm. However, the water depths in both Cases continued to increase hourly and reached a peak of 4.9 m after 56 h. During this last stage, there was minimal (< 1 cm) difference in the water depths.

In summary, the area was entirely inundated in 13 h and 41 min, in 28 h, and in 56 h for inflows of 2,500 m^3/s, 1,200 m^3/s and 600 m^3/s, respectively, in both cases of *n*. The most significant water depth difference between Cases 1 and 2 occurred in the first 2 h after the water depth started increasing, in all three inflow scenarios. The differences in water depth after the first hour of increasing water depth at the Day Weir for inflows of 1,200 m^3/s and 600 m^3/s were 0.49 m and 1.07 m, respectively. Subsequently, the difference showed a downward trend and was zero for the last hour.

Clearly, the difference in *n* had an impact on the relationship between time and water depth in front of the Day Weir during the first two hours of the water starting to rise.

3. Inundated areas

Table 2 shows the percentages of the residential area that were inundated in the 2,500 m^3/s inflow scenario when the water depth in front of the Day Weir reached 1, 2, 3, 4, and 4.9 m. The water depth of 4.9 m corresponds to the maximum height of the weir. In the case of the lowest water depth (1 m at the Day Weir), the total inundated residential area was 66%, and 14% of the residential areas was inundated to a depth of 0.2 to 0.5 m (Level 1). The values for the Level 2 (0.5 to 1.0 m), the Level 3 (1.0 to 2.0 m), the Level 4 (2.0 to 3.0 m) and the Level 5 (3.0 m and more) inundation were 20%, 22%, 8%, and 2%, respectively. When the water depth reached 2 m at the Day Weir, 71% of the residential areas was inundated, with 19% at Level 2, 28% at Level 3, and only 2% at Level 5. There was a significant increase in the percentage of residential areas that were inundated when water reached a depth of 3 m at the Day Weir. Eighty six per cent of housing areas was flooded, with 35% of the residential areas inundated at Level 3, 19% at Level 4,

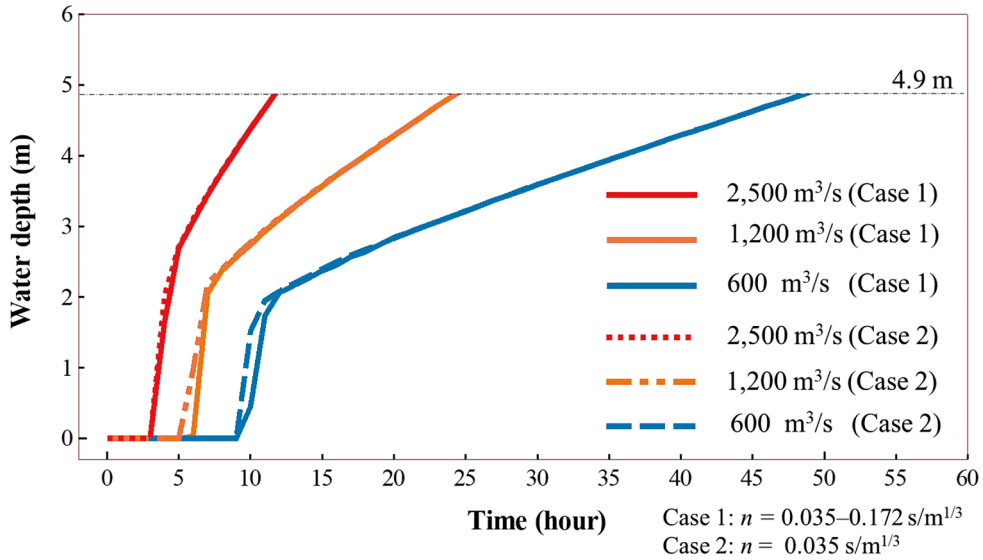

Fig. 7. Relationship between time and water depth in front of the Day Weir

and 9% at Level 5. When the water depth reached 4 m at the Day Weir, 98% of the residential areas was inundated, of which 24% was at Level 3, 35% at Level 4, and 25% at Level 5. When the water depth reached the top of the Day Weir, at a depth of 4.9 m, 99% of the residential areas were inundated, with 15% at Level 3, 25% at Level 4, and 58% at Level 5.

Obviously, floodwater strongly affected the residential areas located in Van Coc Lake. Between 66% and 99% of the residential areas were inundated, dependent on the water depth in front of the Day Weir. When the water depth reached between 1 and 2 m at the Day Weir, residential areas were inundated at Levels 1 to 3, that is, by water of 0.2 to 2.0 m. However, the residential areas were mainly inundated to a depth of 1.0 to 3.0 m when the water depth reached 3 m at the Day Weir. When the water depth reached 4 m at the Day Weir, almost all residential areas were significantly affected by flooding, and 60% of the residential areas were inundated at Levels 4 and 5. In addition, when water overtopped the Day Weir at 4.9 m, all residential areas were inundated, with 58% of the residential areas were under at least 3 m of water.

4. Highest velocity

Figure 8 presents the highest flow velocity at each cell for the 2,500 m^3/s inflow at the Van Coc Gate for two cases of *n*. Zones 1, 2, and 3, located near the Van Coc Gate in the northwest of the area, lie in the highest velocity areas. Zone 1 had velocities of 1.5-1.8 m/s just after the inflow through the Van Coc Gate before moving to Zone 2, where the velocities decreased to 0.6-1.0 m/s. Zone 3 showed a higher velocity than those velocities of Zone 2 because of the effect of elevation. Such high flow velocities may cause erosion of the dike system in the northwest of Van Coc Lake. The remaining areas, that is the majority of the area, had lower flow velocities, from 0.1 to 0.6 m/s. The velocities in front of the Day Weir ranged between 0.1 and 0.4 m/s.

The four different biggest velocity areas (D1, D2, D3, and D4), including cultivated and residential areas,

Table 2. The percentage of the inundated residential area when the water depth in front of the Day Weir reached 1 m, 2 m, 3 m, 4 m, and 4.9 m in the inflow discharge of 2,500 m^3/s

Water depth levels	Unit	The water depth in front of the Day Weir				
		1 m	2 m	3 m	4 m	4.9 m
Total inundated residential area	%	66	71	86	98	99
Water Depth Level 1: 0.2 to 0.5 m	%	14	11	9	4	0
Water Depth Level 2: 0.5 to 1.0 m	%	20	19	13	9	2
Water Depth Level 3: 1.0 to 2.0 m	%	22	28	35	24	15
Water Depth Level 4: 2.0 to 3.0 m	%	8	10	19	35	25
Water Depth Level 5: 3.0 m and more	%	2	2	9	25	58

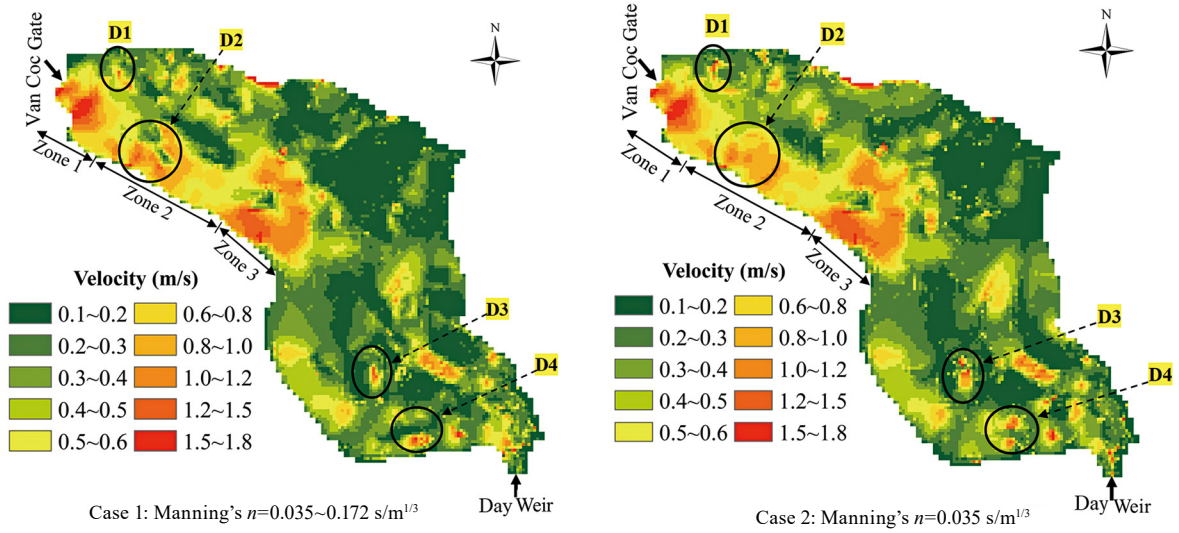

Fig. 8. Highest velocity at each cell in case of the inflow discharge of 2,500 m^3/s at the Van Coc Gate

are shown in Figure 8. These areas were used to compare Cases 1 and 2 of *n*. The velocities at these areas in Case 2 were clearly higher than the velocities in Case 1, especially at the D2 area. That is because the smaller *n* allowed larger longitudinal velocity gradients to appear. In Case 1, *n*-values of 0.172 s/m$^{1/3}$ and 0.035 s/m$^{1/3}$ were used for the residential and cultivated areas located in areas D1, D2, D3, and D4, while the *n*-value of 0.035 s/m$^{1/3}$ was used for all of these areas in Case 2. The *n*-value of the residential areas in Case 1 is 0.137 s/m$^{1/3}$, which is higher than the *n*-value of the residential areas in Case 2. Obviously, *n* is a sensitive parameter in the two-dimensional depth-integrated hydrodynamic model and strongly influences the behavior of flood flows. Hence, the spatially variable *n* was effective for predicting local flow velocities. The remaining areas in Case 1 and Case 2 did not differ significantly regarding flow velocity.

5. Inundated area at each hour

Figure 9 shows the inundated area at each hour after the onset of inflow through the Van Coc Gate for the 2,500 m^3/s scenario with the two cases of *n* (Case 1: *n* = 0.035-0.172 s/m$^{1/3}$ and Case 2: *n* = 0.035 s/m$^{1/3}$). In Case 1, the A1 area was covered by floodwater at the 2nd hour, which did not occur in Case 2. On the other hand, the inundated areas in A2 and A3 in Case 2 were larger than those in Case 1 at the 2nd and 3rd hours, respectively. The reason for this is that the spreading of the inundated areas

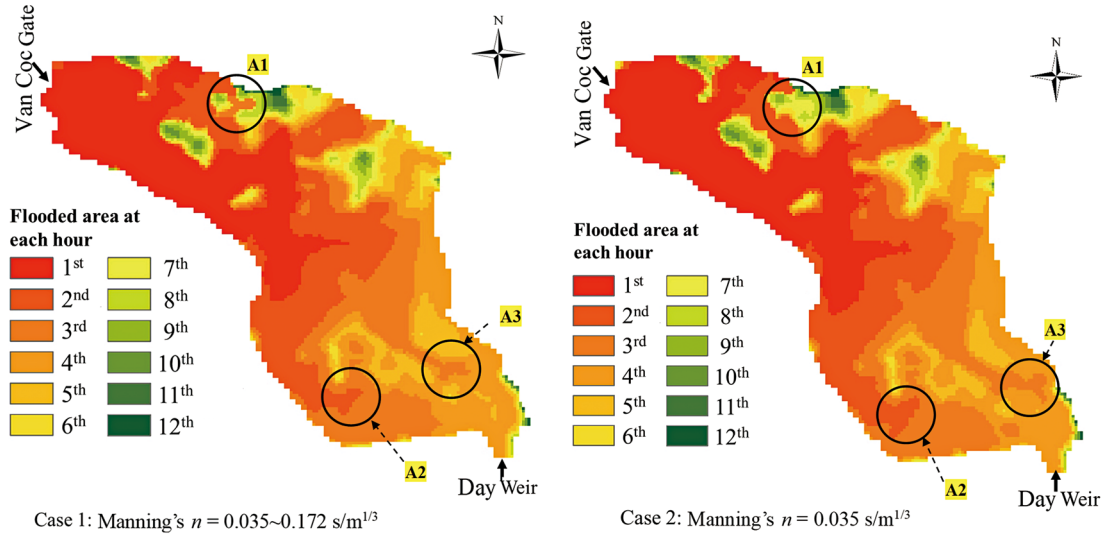

Fig. 9. Flooded area at each hour after the beginning of inflow in the case of the inflow discharge of 2,500 m^3/s at the Van Coc Gate

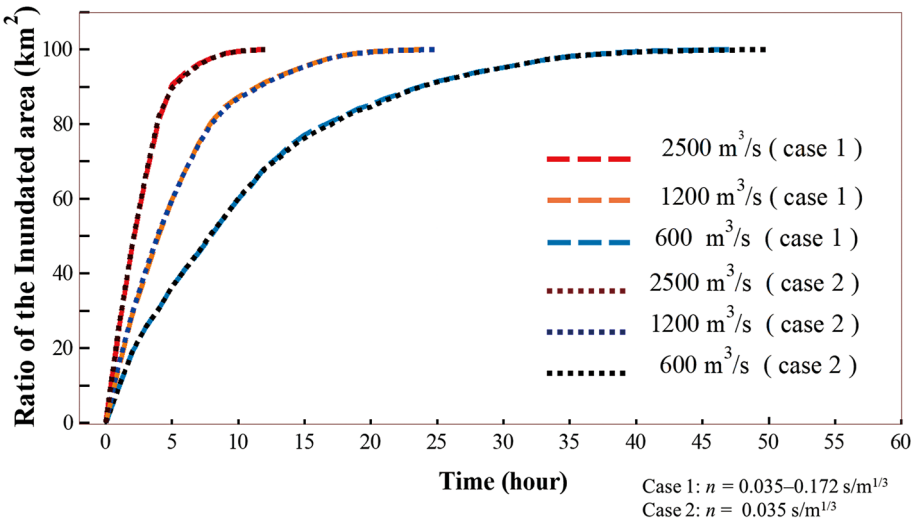

Fig. 10. The relationship between the time after the beginning of inflow and the inundated area

was affected by the different values of the *n*. Flood volumes were spread to the linked depressions using the volume-spreading algorithm in the shallow water equations. Therefore, when the velocities change because of the differing values of *n* in each plot, the flood volume in each plot will also change, which causes the difference in the spreading of the inundated areas in Van Coc Lake.

Figure 10 illustrates the relationship between the time from the onset of inflow and the inundated area for the three inflow discharges of 2,500 m^3/s, 1,200 m^3/s, and 600 m^3/s with two cases of *n* (Case 1: *n* = 0.035-0.172 $s/m^{1/3}$ and Case 2: *n* = 0.035 $s/m^{1/3}$). In the scenario with 2,500 m^3/s inflow and Case 1 for *n*, Figure 10 indicates that the floodwater covered 26.2% of the area after one hour. The floodwater covered 48.2%, 66.1%, and 81.9% in the next three hours. Eventually, 90.2% of the area was inundated after only 5 hours, which was a total of 27.8 km^2. The inundated area spread to the remaining 9.8% of the total area during the next six hours. For Case 2, the inundated area increased from 8.5 km^2 to 25.4 km^2 in the first four hours, which was slightly more than in the Case 1. The difference between the two cases decreased during the next four hours until no difference was found between Cases 1 and 2 after the first eight hours. The differences in inundated areas between Cases 1 and 2 for inflows of 1,200 and 600 m^3/s were small and reached zero in the latter hours of inflow.

Obviously, the different values of *n* affect the spreading of the inundated areas and the *n*-values play an important role in simulating flood flows in the two-dimensional depth-integrated hydrodynamic model. The targeted area will be rapidly covered by floodwater after five hours (approximately 90% of the total area, for both cases of *n*).

Conclusion

In this study, a two-dimensional depth-integrated hydrodynamic model was constructed so as to simulate inundation in Van Coc Lake. A wetting and drying scheme was used to identify the wet and dry areas at each time step. Three inflow rates of 2,500 m^3/s, 1,200 m^3/s, and 600 m^3/s at the Van Coc Gate were considered together with two cases of the Manning's coefficient of roughness *n*: Case 1: *n* = 0.035-0.172 $s/m^{1/3}$; and Case 2: *n* = 0.035 $s/m^{1/3}$. The constructed model was validated in the Red River area using data from Long Bien because there was no recorded profile in Van Coc Lake.

It was concluded that the variation in simulated water depth changes in front of the Day Weir were caused by the difference between the variable and constant values of *n*. The water depth reached the maximum height of the Day Weir (4.9 m) in 13 h and 41 min, 28 h, and 56 h for inflow scenarios of 2,500 m^3/s, 1,200 m^3/s, and 600 m^3/s, respectively. Moreover, floodwater strongly affected the residential areas located in Van Coc Lake causing inundation and major damage to between 66% and 99% of the areas, depending on the water depth in front of the Day Weir. The highest velocity areas are primarily behind the Van Coc Gate with a velocity of 1.5-1.8 m/s in Zone 1, 0.6-1.0 m/s in Zone 2, and 0.8-1.2 m/s in Zone 3. The difference in *n*-values resulted in different velocities, with smaller *n* permitting larger longitudinal velocity gradients to develop. The spread of the inundated areas was also affected by the difference in *n*. Clearly, the *n*-value is an important hydraulic resistance characteristic parameter in the two-dimensional depth-integrated hydrodynamic model and the spatially variable Manning's coefficient of roughness *n* was effective for predicting local flow velocities.

A comprehensive assessment of the hydraulic behavior in the Van Coc Lake area was conducted and these results may assist the Vietnamese Government in issuing early warnings of damage in emergency situations so as to protect the City of Hanoi from flooding from the Red River.

Acknowledgments

The authors appreciate the funding support of JSPS KAKENHI Grant Numbers 23380144, 18H03968 and 17K15347.

References

Abedini, A. A. & Ghiassi, R. (2010) A Three-Dimensional Finite Volume Model for Shallow Water Flow Simulation. *AJBAS*, **4,** 3208-3215.

AHA (ASEAN Coordinating Centre for Humanitarian Assistance on Disaster Management) & JICA (Japan International Cooperation Agency) (2015) *Natural Disaster Risk Assessment and Area Business Continuity Plan Formulation for Industrial Agglomerated Areas in the ASEAN Region, 2013 to 2015. Country Report-Vietnam.*

An, H. et al. (2015) Analysis of an open source quadtree grid shallow water flow solver for flood simulation. *Quat Int*, **384,** 118-128.

Bellos, V. & Tsakiris, G. (2015) Comparing Various Methods of Building Representation for 2D Flood Modelling In Built-Up Areas. *Water Resour Man*, **29,** 379-397.

Bricker, J. D. et al. (2015) On the Need for Larger Manning's Roughness Coefficients in Depth-Integrated Tsunami Inundation Models. *Coast Eng J*, **57,** 1-13.

Brunner, G. (2010) HEC River Analysis System (HEC-RAS) Version 4.1 January 2010.

Caviedes-Voullième, D. et al. (2014) Reconstruction of 2D river beds by appropriate interpolation of 1D cross-sectional

information for flood simulation. *Environ Modell Softw*, **61,** 206-228.

De Doncker, L. et al. (2009) Determination of the Manning roughness coefficient influenced by vegetation in the river Aa and Biebrza river. *Environ Fluid Mech*, **9,** 549-567.

Hu, S. & Kot, S. C. (1997) Numerical Model of Tides in Pearl River Estuary with Moving Boundary. *J Hydraul Eng*, **123,** 9404.

IFRC (International Federation of Red Cross and Red Crescent Societies) (2015) *World Disaster Report - Focus on local actors, the key to humanitarian effectiveness.*

Kalyanapu, A. J. et al. (2009) Effect of land use-based surface roughness on hydrologic model output. *JOSH*, **9,** 51-71.

Kvocka, D. et al. (2015) Appropriate model use for predicting elevations and inundation extent for extreme flood events. *Nat Hazards*, **79,** 1791-1808.

MONRE (Ministry of Natural Resources and Environment) (2012) *Climate change, sea level rise scenarios for Vietnam*. http://www.imh.ac.vn/files/doc/KichbanBDKH/KBBDKH_final May 2012_Part1.pdf [In Vietnamese].

NOAA (National Oceanic and Atmospheric Administration) National Weather Service Public (1993) *NOAA's top global weather, water and climate events of the 20th century.* US National Oceanic and Atmospheric Administration.

Pinho, J. et al. (2015) Comparison between two hydrodynamic models for flooding simulations at River Lima Basin. *Water Resour Manag*, **29,** 431-444.

RRBO (Red River Basin Organization) (2015) *Red-Thai Binh RBO Annual Report*, Hanoi, Vietnam [In Vietnamese].

Smagorinsky, J. (1963) General circulation experiments with the primitive equations. *Mon Weather Rev*, **91,** 99.

Tabata, T. et al. (2013) Numerical analysis of convective dispersion of pen shell *Atrina pectinata* larvae to support seabed restoration and resource recovery in the Ariake Sea, Japan. *Ecol Eng*, **57,** 154-161.

Uchiyama, Y. (2004) Modeling wetting and drying scheme based on an extended logarithmic law for a three-dimensional sigma-coordinate coastal ocean model. *Rep Port Airpt Res Inst*, **43,** 3-21.

Vietnamese Government (2011) 04/2011/ND-CP: *Abolish the use of flooding diversion areas and flooding diversion system of Day River, Vietnam*. http://www.tongcucthuyloi.gov.vn/He-thong-van-ban/Van-ban-phap-luat/docid/566/nghi-dinh-04-2011-nd-cp-thuc-hien-bai-bo-viec-su-d [In Vietnamese].

Vietnamese Government (2014) 1821/QD-TTg: *Planning approval flood prevention and Day River dike system, Vietnam*. http://vanban.chinhphu.vn/portal/page/portal/chinhphu/hethongvanban?mode=detail&document_id=176718 [In Vietnamese].

Vietnamese Government (2016) 257/QD-TTg: *Planning for flood prevention and Red-ThaiBinh River dike system, Vietnam*. http://vanban.chinhphu.vn/portal/page/portal/chinhphu/hethongvanban?class_id=2&mode=detail&document_id=183476 [In Vietnamese].

Wu, W. & Lin, Q. (2015) Advances in water resources A 3-D implicit finite-volume model of shallow water flows. *Adv Water Resour*, **83,** 263-276.